Mapping Global Angular Transitions of Proteins in Assemblies Using Multiple Extrinsic Reporter Groups†

Thomas P. Burghardt* and Katalin Ajtai
Department of Biochemistry and Molecular Biology, Mayo Foundation, Rochester, Minnesota 55905
Received May 29, 1991; Revised Manuscript Received August 7, 1991

ABSTRACT: The fluorescence polarization intensities from fluorescent probes and the electron paramagnetic resonance spectra from spin probes, specifically modifying elements of a biological assembly such as myosin sulfhydryl 1 (SH1) in muscle fibers, are interpreted in terms of probe order parameters using a model-independent method. The probe order parameters are related to each other by an Euler rotation of coordinates. We use this relationship to link the sets of order parameters from the different probes and in so doing create a system of equations that can be solved using only the information available from the experimental data. The solution yields the Euler angles relating the different probe coordinate frames and a larger set of probe order parameters than can be directly detected experimentally. The Euler angles are used to display the relative orientation of the probe molecular frames. The order parameters give rise to probe angular distributions that are at the theoretical limit of resolution. We demonstrate the utility of this analytical method by investigating the rotation of myosin SH1 from its orientation in rigor upon the binding of the nucleotide MgADP to the myosin cross-bridge. Our findings, discussed in the accompanying paper, suggest that the rigor-to-MgADP cross-bridge angular transition consists predominantly of a rotation about the hydrodynamic axis of symmetry of the cross-bridge, i.e., its torsional degree of freedom [Ajtai, K., Ringler, A., & Burghardt, T. P. (1992) *Biochemistry* (following paper in this issue)].

The investigation of the molecular mechanism of muscle contraction sometimes involves the use of direction-reporting extrinsic probes that can chemically modify selected side chains on the muscle proteins of interest. If the probe is rigidly attached to the protein so that it does not rotate independently, then direction-reporting signals from the probe can supply information related to the angular distribution of the protein in the vicinity of its modified side chain. We use two experimental techniques to investigate probe orientation, electron paramagnetic resonance (EPR) and fluorescence polarization. Both techniques detect the orientation of an intrinsic coordinate frame fixed in the probe molecule (Burghardt & Ajtai, 1990).

In the muscle we focused our investigation on the myosin molecule by placing probes on the reactive sulfhydryls (SH1 or SH2) located in the head region of the protein. The myosin head, or cross-bridge, interacts with the actin filaments and hydrolyzes ATP during muscle shortening. It is thought that the myosin cross-bridge uses the chemical energy liberated from ATP hydrolysis to generate force at the actomyosin interface to make the muscle shorten. The mechanism by which myosin accomplishes this transduction of energy is a central question of muscle research. The idea that this mechanism may involve a rotation of the cross-bridge while it is actin bound such that the myosin rolls on the actin filament was suggested years ago (Huxley, 1969; Huxley & Simmons, 1971), but the experimental verification of a changing cross-bridge orientation has been controversial.

The controversy surrounding the rotating cross-bridge model of contraction is due to part to the apparent contradictions in the conclusions drawn from the direction-reporting probes (Burghardt & Ajtai, 1990). Although it seems now certain that the extrinsic probes of the cross-bridge report that the cross-bridge assumes various orientations relative to actin, there are lingering questions about why some probes reported large angular displacements of the cross-bridge (Borejdo et al., 1982; Burghardt et al., 1983) while others reported nearly undetectable orientation changes (Cooke et al., 1982; Fajer et al., 1990). We have shown that the differing orientations of the probes within the cross-bridge molecular frame contribute to the probes ability it detect cross-bridge orientation changes. We showed this by spectroscopically varying the molecular frame orientation of the transition dipoles of several fluorescent probes and determined that some probe molecular frame orientations of a single probe are more sensitive than others (Ajtai & Burghardt, 1987). It seems likely that transition dipoles from cross-bridge rotation-insensitive probes point along the axis of cross-bridge rotation while dipoles from rotation-sensitive probes are more perpendicular to this axis of rotation. This possibility may be tested quantitatively by the method we introduce below.

Assuming that the myosin cross-bridge is a rigid body, then its rotation causes a similar rotation of each probe on its surface. The angular distributions of the individual probes are constrained by the requirement that they must reflect the rotation of their common host. How well the observed probe distributions fit these constraints, when the cross-bridge undergoes a physiological state change, gives a quantitative measure of how well the experimental data agree with the original assumption of a rigid body rotation. Consequently, we will be able to decide for the probes we choose to study whether or not the cross-bridge behaves like a rigid body. Additionally, by the application of this formalism we (i) enhance the angular resolution of each of the probe distributions to the theoretical limit, (ii) find a best choice for the extent of cross-bridge rotation during a physiological state change of the fiber, and (iii) find the relative orientation of the probe-fixed reference frames.

† This work was supported by the National Science Foundation (DMB-8819755), the National Institutes of Health (1 R01 AR 39288-01A1), the American Heart Association (Grant-in-Aid 900644), and the Mayo Foundation. Computer time was furnished by the Research Computer Facility of the Mayo Foundation. T.P.B. is an established investigator of the American Heart Association.
* To whom correspondence should be addressed.

0006-2960/92/0431-200$03.00/0

We implement this formalism by combining data from different probes of the myosin cross-bridge using model-independent order parameters. The order parameters define the probe angular distribution function N when it is expanded in a sum of appropriate orthonormal angular functions with order parameter coefficients. This description of N is general and can be applied to either EPR or fluorescence polarization techniques for probe order measurement (Burghardt, 1984; Burghardt & Thompson, 1985).

For our purposes, the various probes on a protein side chain differ from each other only in their orientation relative to a reference frame fixed in the protein. Consequently, we must be able to relate order parameters from different probes by a rotation of coordinates. It follows then that there are connections among the order parameters from different probes that can be formulated as a system of equations with order parameters, and the angles relating order parameters from different probes, as variables. Requiring that any rigid rotation of the modified protein results in a similar rotation of all of the probes, and using information from the experimental measurement of EPR and fluorescence polarization spectra, we obtain a system of equations for the unknown order parameters. The number of probes and the experimental conditions are chosen so that the number of experimental observations is larger than the number of unknowns. The unknowns are determined by minimizing the square of the differences between the appropriate theoretical and experimentally observed parameters [least-squares minimization, see Strang (1986)].

In the accompanying paper, we describe the application of this formalism to three probes of myosin SH1 (Ajtai et al., 1992). These probes are the spin labels [^{15}N,^{2}H]MTSL and IPSL and the fluorescent probe 15IA. The 15IA data enter the calculation as three data sets since we include data at three wavelength points along the probe's excitation polarization spectrum. The results demonstrate the utility of the method.

THEORY

A. Model-Independent Description of the Probe Angular Distribution. The analytical function N is the angular distribution of probes in a biological assembly. N describes the distribution of probe-fixed coordinate frames relative to a laboratory-fixed coordinate frame. A rotation of coordinates, using the Euler angles α, β, and γ, denoted collectively by Ω, relates the lab frame to the probe frame as shown in Figure 1 for the case of a spin label (Davydov, 1963). It is useful to expand $N(\Omega)$ in terms of the Wigner functions $\mathbf{D}^{j}_{m,n}(\Omega)$ that form a complete orthogonal set of functions on the domain of Euler angles Ω_0, where $0 \leq \alpha_0 \leq 2\pi$, $0 \leq \beta_0 \leq \pi$, and $0 \leq \gamma_0 \leq 2\pi$, such that

$$N(\Omega) = \sum_{j=0}^{\infty} \sum_{m,n=-j}^{j} a^{j}_{m,n} \sqrt{\frac{2j+1}{8\pi^2}}\, \mathbf{D}^{j}_{m,n}(\Omega) \qquad (1)$$

The parameter $a^{j}_{m,n}$ is an order parameter of rank j, and it represents the contribution to N of the (j,m,n)th component of the set of functions $\mathbf{D}^{j}_{m,n}$. The orthogonality of the Wigner functions imply that

$$\int_{\Omega_0} \mathbf{D}^{j*}_{m,n} \mathbf{D}^{j'}_{m',n'}\, d\Omega = \frac{8\pi^2}{2j+1} \delta_{jj'} \delta_{m,m'} \delta_{n,n'} \qquad (2)$$

where an asterisk (*) means complex conjugate and $\delta_{k,k'}$ is the Kronecker delta.

The order parameters are unknowns that are determined experimentally by analysis of fluorescence polarization or EPR data (Burghardt & Thompson, 1985; Burghardt & French, 1989). We showed that the number and rank of order parameters that can be estimated from EPR exceeds that obtainable from fluorescence polarization. Fluorescence polarization is sensitive to order parameters of rank $j \leq 4$, while EPR is sensitive to ranks $j = 0, 2, 4, \ldots$ [there are some exceptions to these selection rules see Burghardt (1989)]. In practice this means that generally a spin probe angular distribution has higher resolution than a fluorescent probe angular distribution.

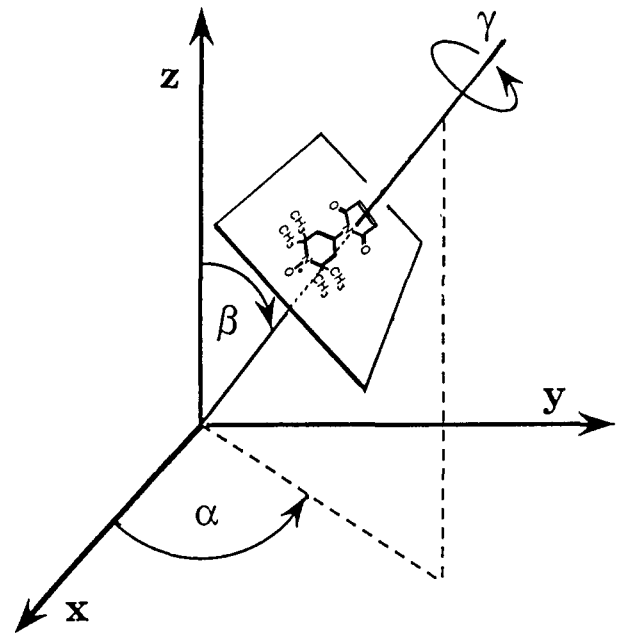

FIGURE 1: Euler angles for a spin probe modifying a biological assembly. The Euler rotation takes the laboratory frame to the principal magnetic frame of the spin probe. In this case the z-axis of the principal magnetic frame is perpendicular to the plane of the ring containing nitrogen. In a system having symmetry that eliminates α dependence in the probe angular distribution, such as a muscle fiber, multiple probes would be evenly distributed in their α angle while each probe would have identical β and γ angle values.

B. Relationship among Different Probe Order Parameters. While fluorescence polarization and EPR data are quantitated in terms of order parameters, the values of the order parameters from the different probes are not interchangeable when they describe their probe angular distribution. A rotation can always be found, however, to relate any two sets of order parameters such that

$$a^{j}_{m,n}(\mathrm{II}) = \sum_{k=-j}^{j} a^{j}_{m,k}(\mathrm{I}) \mathbf{D}^{*j}_{k,n}(\Omega_i) \qquad (3)$$

where Ω_i represents $(\alpha_i,\beta_i,\gamma_i)$ relating probe I to probe II.

Equation 3 shows that, under a rotation of molecular coordinate frames, the values of the order parameter indices j and m are conserved, implying that order parameters transform under molecular coordinate frame rotation into order parameters of the same rank j and m index. The conservation of the j index simplifies our problem of relating the probe order parameters since we may consider each rank independently. The conservation of the m index has special significance for the muscle fiber system since we have experimental evidence that the angular distribution of probes on SH1 is unchanged by rotation of the fiber about the fiber axis (Burghardt et al., 1983). This fiber symmetry implies that $a^{j}_{m,n} = a^{j}_{0,n}\delta_{m,0}$ and, because of m index conservation, that this relationship holds for any probe on SH1. Consequently, for probes of SH1 we may limit our consideration to order parameters of the form $a^{j}_{0,n}$. In systems not similar in this way to the muscle fiber,

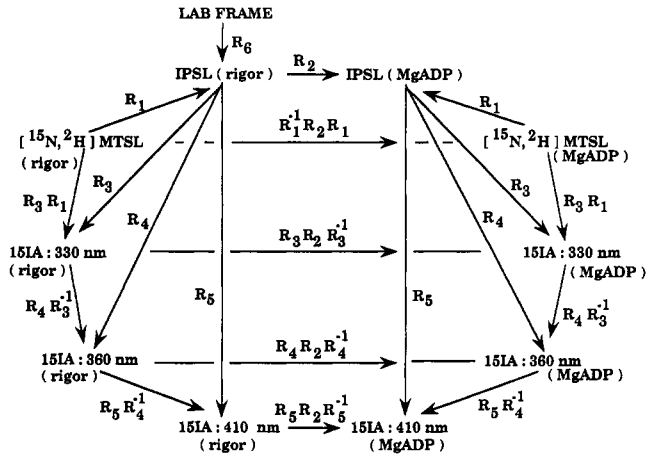

FIGURE 2: Relationships among the probes of myosin SH1 for fibers in rigor and in the presence of MgADP. Rotation operators R_i connect probe-fixed reference frames that differ from each other by an Euler rotation. Rotation operator R_2, or its similar operator $R_iR_2R_i^{-1}$, corresponds to the rigor-to-MgADP transition.

we must consider the order parameters for each m index value separately.

C. Setting Up the Problem. We want to find the order parameters of three probes of myosin SH1 in fibers, for fibers in rigor and in the presence of MgADP. The probes of SH1 that we are interested in are the spin labels [^{15}N,^{2}H]MTSL and IPSL and the fluorescent label 15IA. We measured the excitation polarization spectrum from 15IA-labeled fibers and include data from three different excitation wavelength points in our calculation. In this case, fluorescence polarization ratios at excitation wavelengths λ_{ex} = 330, 360, and 410 nm are included and are equivalent to data from three independent probes of SH1. We consider then five different probes in two physiological states corresponding to 10 independent data sets.

The logic used to relate the data sets is shown in Figure 2. Each rotation operator R_i can be represented as a function of three Euler angles. The rotation operators are defined such that the tip of the arrow, connecting two sets of order parameters, points to the result of applying the rotation operator to order parameters at the base of the arrow. As shown in Figure 2, the rigor-to-MgADP angular transition is described by rotation operator R_2 or a related operator given by the similarity transformation $R_iR_2R_i^{-1}$.

Adding a new probe to our calculation requires that we introduce a new rotation operator, R_i, or equivalently three new Euler angles that must be determined in the complete solution to the problem. If the new probe is fluorescent, then we will show subsequently that six or more observable (known) quantities are offset by the unknown Euler angles so that the number of constraints increases by at least three. By increasing the number of constraints on the unknown order parameters, we increase the likelihood of finding the best global solution. New spin labels add even more constraints than the fluorescent labels. Unfortunately, the constraints and unknowns also increase the computer time needed to find the best global solution. Our choice of five probes was the largest set of probes that we could analyze within a reasonable amount of computer time.

We relate the probe order parameters to each other with rotation operators R_i that represent a single Euler rotation through angles Ω_i. This is a model-dependent assumption about the relationships among the probes. An alternative assumption is that the Euler rotation angles are distributed over a domain of values. The latter assumption introduces more unknowns to the problem (that can be calculated since the problem is overdetermined), but we do not pursue this option further since the former assumption produces reasonable solutions.

D. Relationship between Observables and Order Parameters. The EPR spectrum, $E(H)$, is interpreted in terms of order parameters using

$$E(H) = \sum_{i}^{i_{max}} a_i g_i^{EPR}(H) \tag{4}$$

where H is the strength of the Zeeman field, a_i (representing $a^j_{m,n}$) is an order parameter, $g_i^{EPR}(H)$ is a basis spectrum, and i_{max} is the total number of order parameters contributing significantly to the EPR spectrum. The significant order parameters are usually those parameters $a^j_{0,n}$ of rank $0 \leq j \leq 16$. Previously, the linear relationship between a_i and $E(H)$ was exploited to compute the linear least-squares approximately of the best fitting a_i's directly from the EPR spectrum (Burghardt & Thompson, 1985; Burghardt & French, 1989). In our present method, these equations are solved simultaneously with other equations constraining the order parameters are described below.

Fluorescence polarization data are the intensities $F(\psi,\chi,\lambda_{ex},\lambda_{em})$, where ψ and χ are angles relating the orientation of the excitation and the emission polarizers relative to the laboratory frame, and λ_{ex} and λ_{em} refer to the wavelength of the excitation and emission light. The intensities are related linearly to the order parameters by

$$F(\psi,\chi,\lambda_{ex},\lambda_{em}) = \sum_i a_i g_i^{FLS}(\psi,\chi,\lambda_{ex},\lambda_{em}) \tag{5}$$

The dependence of g_i^{FLS} on the parameters ψ, χ, λ_{ex}, and λ_{em} was described for the general case (Burghardt, 1984). We have already noted that the sum over i in eq 5 is finite and should include order parameters of rank $j \leq 4$. This is unlike the sum over i in eq 4 where all even rank order parameters contribute to $E(H)$.

It is customary to use the ratios defined below to summarize the fluorescence polarization data:

$$P_{\parallel} = \frac{F(0°,0°) - F(0°,90°)}{F(0°,0°) + F(0°,90°)} \tag{6}$$

$$P_{\perp} = \frac{F(90°,90°) - F(90°,0°)}{F(90°,90°) + F(90°,0°)} \tag{7}$$

$$Q_{\parallel} = \frac{F(0°,0°) - F(90°,0°)}{F(0°,0°) + F(90°,0°)} \tag{8}$$

where we suppressed the λ_{ex} and λ_{em} dependence in F. The use of ratios eliminates the necessity of measuring absolute light intensities in these experiments. The linear relationship between order parameters and the observable quantities $P_{\parallel}$, $P_{\perp}$, and $Q_{\parallel}$ is preserved by rearranging the ratios into the forms

$$(P_{\parallel} - 1)F(0°,0°) + (P_{\parallel} + 1)F(0°,90°) = 0 \tag{9}$$

$$(P_{\perp} - 1)F(90°,90°) + (P_{\perp} + 1)F(90°,0°) = 0 \tag{10}$$

$$(Q_{\parallel} - 1)F(0°,0°) + (Q_{\parallel} + 1)F(90°,0°) = 0 \tag{11}$$

E. Order Parameters of Rank j = 1 and 3. It is noteworthy that the data $P_{\parallel}$, $P_{\perp}$, and $Q_{\parallel}$ do not contain all of the information that can be obtained from a fluorescence polarization experiment. Inspection of eqs A4–A9 in the Appendix show that order parameters of ranks j = 1 and 3 contribute to the fluorescence intensity only when ψ and χ are not equal to 0° or 90°. This condition is not met by $P_{\parallel}$, $P_{\perp}$, and $Q_{\parallel}$, and a more general set of ratios must be defined to take advantage

Table I: Molecular Frame Euler Angle Symmetries[a]

α_1	β_1	γ_1	$\alpha_1 + \pi$	β_1	γ_1	α_1	β_1	γ_1
α_2	β_2	γ_2	α_2	β_2	γ_2	α_2	β_2	γ_2
α_3	β_3	γ_3	α_3	β_3	γ_3	$\alpha_3 + \pi$	$\pi - \beta_3$	$\pi - \gamma_3$
α_4	β_4	γ_4	α_4	β_4	γ_4	α_4	β_4	γ_4
α_5	β_5	γ_5	α_5	β_5	γ_5	α_5	β_5	γ_5
α_1	β_1	γ_1	α_1	β_1	γ_1	$\pi - \alpha_1$	β_1	$\pi - \gamma_1$
α_2	β_2	γ_2	α_2	β_2	γ_2	$\pi - \alpha_2$	β_2	$\pi - \gamma_2$
α_3	β_3	γ_3	α_3	β_3	γ_3	$\pi - \alpha_3$	β_3	$-\gamma_3$
$\alpha_4 + \pi$	$\pi - \beta_4$	$\pi - \gamma_4$	α_4	β_4	γ_4	$\pi - \alpha_4$	β_4	$-\gamma_4$
α_5	β_5	γ_5	$\alpha_5 + \pi$	$\pi - \beta_5$	$\pi - \gamma_5$	$\pi - \alpha_5$	β_5	$-\gamma_5$
α_1	β_1	$\gamma_1 + \pi$	α_1	$\pi - \beta_1$	$\pi - \gamma_1$			
$\alpha_2 + \pi$	β_2	$\gamma_2 + \pi$	$-\alpha_2$	β_2	$-\gamma_2$			
$\alpha_3 + \pi$	β_3	γ_3	$-\alpha_3$	β_3	$-\gamma_3$			
$\alpha_4 + \pi$	β_4	γ_4	$-\alpha_4$	β_4	$-\gamma_4$			
$\alpha_5 + \pi$	β_5	γ_5	$-\alpha_5$	β_5	$-\gamma_5$			

[a] For any value of $(\alpha_i,\beta_i,\gamma_i)$ where $i = 1, ..., 5$ the least-squares minimization X^2 are identical for each of the eight sets of Euler angles identified above. The symmetries are degeneracies in X^2 that exist for the order parameters considered in our application. This list is not necessarily all of the degeneracies could that exist.

of this feature of the fluorescence polarization signal. In model calculations discussed subsequently in section J, we find that the measurement of fluorescence intensities when ψ and χ equal 0, 30°, 60°, or 90° (to make 15 independent ratios from 16 intensities) is sufficiently general to enable one to determine the $j = 1$ and 3 order parameters.

F. Application to Experimental Data. When order parameter $a^j_{m,n} = a^j_{0,n}\delta_{m,0}$, as in our application to muscle fibers, each rank j corresponds to $2j + 1$ parameters since $-j \leq n \leq j$. Rank $j = 0$ corresponds to the random distribution component of the probe angular distribution. In our application, we consider order parameters of rank $j = 0, 2, 4, ..., 16$. Order parameters of odd rank are eliminated from consideration because neither EPR nor fluorescence polarization depends upon them (except for fluorescence polarization under the circumstances discussed in the model calculation, see section J). We also do not consider parameters of higher even rank than $j = 16$ because we have sufficient information from the EPR and fluorescence polarization data to find a global solution without them and because the computation time required for including them is prohibitive. By not including every possible order parameter in our problem, we do not necessarily inhibit our ability to find the best global solution since the order parameters of different ranks are independent.

The equations determining the order parameters combine the constraints of eq 3 with the constraints of eqs 4 and 9–11. We begin by choosing the set of unknown order parameters. It will become clear below that it is sufficient to choose as unknowns the spin probe order parameters. These unknowns are the parameters that make up the set $\{a^j_{0,n}\}$ for $j = 0, 2, 4, 6$, with $-j \leq n \leq j$, and for $j = 8, 10, ..., 16$, with $n = 0, 2, 4$. Each probe has a separate set of order parameters.

The spin probe order parameters are related to each other via eq 3 and to the experimentally observed EPR spectra via eq 4. Order parameters of rank $j \geq 8$ are restricted only by eq 4 because the computation time required to calculate the appropriate rotation matrices from eq 3 for these high rank parameters is prohibitive. In our computation, we arrange the spin probe order parameters into a $n \times 1$ array, $\mathbf{u}$, and the known quantities (the EPR spectral intensities) into a $m \times 1$ array, $\mathbf{k}_s$. The relationship between $\mathbf{u}$ and $\mathbf{k}_s$ is linear such that

$$\mathbf{Mu} = \mathbf{k}_s \tag{12}$$

where $\mathbf{M}$ is an $m \times n$ matrix with elements made up from the appropriate rotation matrices $\mathbf{D}^{j*}_{l,l}$ from eq 3 and the basis spectra $g^{EPR}_l(H)$ from eq 4. For two spin probes $m > n$ so that unknowns $\mathbf{u}$ can be determined exclusively from EPR data, however, we want to also include the information from the fluorescent probes.

The fluorescent probe order parameters are linearly related to the spin probe order parameters by eq 3. The fluorescent probe order parameters are also related to the observed intensity ratios by eqs 9–11. By these two relationships, the unknown spin probe order parameters are linearly related to the polarization intensities such that

$$\mathbf{Gu} = \mathbf{k}_f \tag{13}$$

where the unknowns $\mathbf{u}$ are identical to those in eq 12 and the known polarization intensities are contained in the $l \times 1$ array $\mathbf{k}_f$. We derive in the Appendix the components of $\mathbf{k}_f$ and the $l \times n$ matrix $\mathbf{G}$ that are appropriate for our application. All of the constraints from EPR and fluorescence polarization experiments constrain identical unknowns so that

$$\begin{pmatrix} \mathbf{M} \\ \mathbf{G} \end{pmatrix} \mathbf{u} = \begin{pmatrix} \mathbf{k}_s \\ \mathbf{k}_f \end{pmatrix} \tag{14}$$

The $m + l$ constraints on $\mathbf{u}$ in eq 14 represent more equations than unknowns if $m + l > n$. This problem is solved by finding the best solution for $\mathbf{u}$ using a weighted least-squares protocol (Strang, 1986).

G. Technical Details. We solved for the Euler angles and unknown order parameters of the probe angular distribution using a weighted least-squares minimization with equality and inequality constraints routines (Haskell & Hanson, 1979). The input to the program included eq 14 and constraints on the minimum and maximum values of the order parameters (the inequality constraints). The inequality constraints are from the theoretical limitations on the order parameters as described previously (Burghardt & Thompson, 1985).

The values of the unknown order parameters are given directly by the weighted least-squares minimization routine. The Euler angles are nonlinear parameters in the equations. We computed the weighted least-squares value, X^2, for every point on a 15-dimensional grid of points made up from the Euler angles (five probes in two states corresponding to 15 Euler angles). The best choice for the Euler angles was that which minimized X^2.

All of the least-squares solutions to the system of equations could be found without trying every point on the 15-dimensional grid of Euler angles. This is because certain changes in one or more of the Euler angles do not change the value of X^2. The Euler angle translations that do not effect X^2 are listed in Table I. We restricted the domain of the search

through the Euler angle variables to take advantage of this ambiguity to reduce the amount of computer time necessary to try all possibilities. This implies that each solution corresponds to a set of several equivalent solutions. The selection of a particular solution is based on separate criteria appropriate for a particular application. The criteria for our muscle fiber application are discussed in the accompanying paper (Ajtai et al., 1992).

H. Probe Orientation Distribution. The orientation distribution of a cross-bridge bound probe in a muscle fiber, denoted by N, depends on the Euler angles α, β, and γ (Davydov, 1963). Euler angles α and β are the probe azimuth and polar angles relative to the fiber axis of symmetry, and γ is the torsion angle (see Figure 1). The muscle fiber axis is a symmetry axis so that angle α can be ignored. The probe orientation distribution is computed from the order parameters with the relation

$$N(\beta,\gamma) = \sum_{j=0}^{j_{max}} \sum_{n=-j}^{j} a^j_{0,n} \sqrt{\frac{2j+1}{8\pi^2}} D^j_{0,n} \qquad (15)$$

Equation 15 is a simplified version of eq 1 reflecting the α independence of the cross-bridge bound probe distribution (since $a^j_{0,n}$ appears, not $a^j_{m,n}$) and the finite limit on the rank of the known order parameters (j_{max} replaces ∞). We can summarize the results by presenting three-dimensional representations of N. In these plots, β and γ are the independent variables and N is the dependent variable. Domains in β and γ of large (small) N represent regions of high (low) probe orientation density. We also use two-dimensional representations of the probe distribution calculated by averaging $N(\beta,\gamma)$ over either β or γ [see Ajtai et al. (1992)].

I. Relationship of the Lab- to Probe-Fixed Reference Frame. As indicated above, we can determine the relationship among the probe-fixed reference frames. This information pertains only to relative orientations and does not fix the probe orientation in the laboratory frame. The relationships between the laboratory frame and the probe frames are different than the relationships among the probe frames since the former is not related by a single Euler rotation but is a distribution of rotations. The distribution of rotations is given by N in eq 1. Nevertheless, it is reasonable to attempt to estimate the Euler rotation from the lab frame to the most probable orientation of the probe-fixed frame. We attempted this calculation by rotating a lab-fixed frame to the probe frame of IPSL in rigor and then subsequently rotating this frame to every other probe frame using the rotations R_i. The initial rotation to IPSL in rigor, designated R_6 (see Figure 2), is an Euler rotation with angles Ω_6. The angles represented by Ω_6 were varied over all possible values, and, at each choice of Ω_6, the overlap of the rotated lab frame with the appropriate probe probability distribution function was computed. We chose the best value for Ω_6 by maximizing the sum of the overlaps from each probe distribution.

We consider the findings of this computation a suggestion for Ω_6 since a more rigorous estimate could be made only by knowing the real probe distribution function given by N in eq 1. The distribution functions we must use are based on eq 15 where only a subset of the order parameters are known.

J. Model Calculations. We checked the computer program written to implement the methods introduced here for its ability to locate the correct solution for Euler angles and unknown order parameters. We did this with model calculations in which order parameters calculated from a Gaussian distribution of probes were rotated to various orientations with randomly selected Euler angles. This complete set of order parameters so generated gives the theoretical values for all of the unknown order parameters in our calculation. The theoretical order parameters pertaining to spin labels are used to compute the EPR spectra that are input to the computer program. The order parameters pertaining to fluorescence probes are used to calculate theoretical polarization intensities that are also input to the program to simulate a real application.

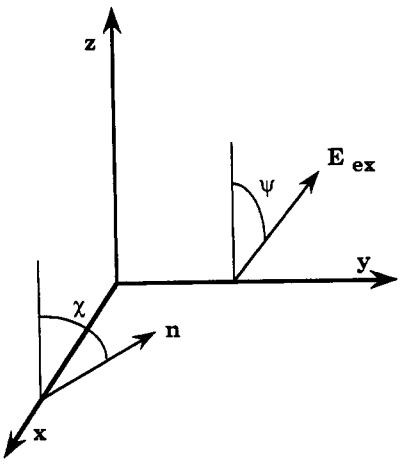

FIGURE 3: Fluorescence polarization experiment where emitted light is collected at 90° from the excitation beam. Exciting light propagating along the y-axis has polarization $\vec{E}_{ex}$. Emitted light is collected from along the x-axis with linear polarization (after passing through a polarizer) $\vec{n}$. In our muscle fiber experiments, the fiber axis was always oriented along the z-axis.

When the program was allowed to search through the 15-dimensional Euler angle space, as it would in a real application, the program identified all 15 of the correct Euler angles by indicating the X^2 for the correct choices to be a factor of 10^4 smaller than that for the next best choices. This solutions also computed all of the order parameters to within ~1% of their theoretical values. The excellent correlation between the theoretical and calculated order parameters and the clear ability of the method to identify the correct Euler angles gives us confidence that our program works as it is intended.

Another version of our program extends the resolution of the standard program by including contributions of order parameters of rank $j = 1$ and 3. This extension requires additional data from the fluorescent probes of a form briefly described as follows. We identify the fluorescence intensities by wavelength (excitation, λ_{ex}, and emission, λ_{em}) and by the orientation of the polarization of the electric fields of the exciting and emitted light. If a fiber axis is oriented along the lab frame z-axis, the exciting light is propagating along the lab y-axis, and the emitted light is analyzed and detected along the lab x-axis as shown in Figure 3, then fluorescence intensities are uniquely defined by $F(\psi,\chi,\lambda_{ex},\lambda_{em})$, where ψ is the angle the electric field of the exciting light ($\vec{E}_{ex}$) makes with the lab z-axis and χ is the angle the electric field of the emitted light ($\vec{n}$) makes with the lab z-axis after passing through the emission polarizer. Fluorescence intensities where ψ or χ are 0° or 90° do not depend on the rank $j = 1$ or 3 order parameters (see eqs A4–A9). We must have other intensities in our data set to detect the contribution from the $j = 1$ and 3 order parameters. We choose to include the intensities from ψ or χ equal to 30° or 60° in addition to the intensities in the standard measurements.

We performed a model calculation identical to that described above but now extended to include the $j = 1$ and 3 order parameters. The input data set included the fluorescence polarization ratios resulting from ψ and χ equal to 0°, 30°,

60°, and 90° (amounting to 16 intensities that are combined into 15 ratios). The extended program was equal to the standard program in its ability to identify the correct Euler angles and unknown order parameters. This suggests that a significant angular resolution enhancement may be obtained by extending the data set measured from the fluorescent probes. The importance of this result will be investigated in future work.

Discussion

The role of cross-bridge orientation in muscle contraction has been thoroughly investigated experimentally with the use of extrinsic direction-reporting probes attached to the myosin head [for a review, see Burghardt and Ajtai (1990)]. The extrinsic probes are site selective on myosin S1, not detrimental to protein or muscle function, and the signals originating from EPR and fluorescent probes have a high signal-to-noise ratio that are rich in probe orientation information.

Despite these advantages, fluorescent and EPR probe studies of cross-bridge orientation produced contradictory interpretations of the data. The extension of these probe studies, using a global approach for mapping probe angular movements, is introduced to explain quantitatively the conflicting findings of the probes. It is generally understood that no single probe can investigate all three angular degrees of freedom in which a myosin cross-bridge (or generally a protein in a biological assembly) can move. The experimental techniques (as in fluorescence polarization and EPR) or the precision with which the technique is used cannot compensate for the unfavorable alignment of the probe axis with the principal axis of rotation of the cross-bridge or the equivalence of a physical probe rotation with a rotational ambiguity of the signal. Although the possibility of obtaining EPR spectra from oriented samples at high microwave frequencies (i.e., at Q-band compared to the more commonly used X-band) could permit enhanced resolution of spin probe orientation changes (Robinson et al., 1985).

With these limitations in mind, it is clear that our goal is to gain insight into the global motion of the cross-bridge by combining the information from different complementary techniques and/or different probes. This combination of data is more able to eliminate ambiguity or accidental degeneracy in detecting probe rotation. The results of the application of our analytical technique to specific probes of the myosin cross-bridge are described in the accompanying paper (Ajtai et al., 1992).

Our method is generally applicable to biological assemblies where multiple specific probes can be introduced into the oriented sample. The most important advantages of the method are that (i) ambiguities in the angular distribution of the direction-reporting probes are reduced or eliminated, (ii) the angular resolution of both fluorescent and spin probe distributions are significantly enhanced, and (iii) the combination of probe data sets yields the Euler angles relating the probe molecular frames on the protein surface.

We demonstrate advantage (i) with the spin probe distributions plotted in the accompanying paper. Previous to this work, we showed that the analysis of EPR spectra from individual probes yielded a probe distribution that was unchanged under coordinate translations $(\beta,\gamma) \rightarrow (\pi-\beta,\gamma)$, $(\beta,\pi+\gamma)$, $(\pi-\beta,\pi+\gamma)$, $(\beta,-\gamma)$, $(\pi-\beta,-\gamma)$, $(\beta,\pi-\gamma)$, and $(\pi-\beta,\pi-\gamma)$ (Burghardt & French, 1989). These symmetries of the probe angular distribution represent ambiguities that are introduced by the limitations of the experimental technique used to measure order parameters. Our method of combining data sets of different probes removes some (all of them if $j = 1$ and 3 order parameters are included) of these ambiguities so that the real probe distribution can be observed.

We demonstrate advantage (ii) with the fluorescent probe distributions plotted in the accompanying paper. The angular resolution is enhanced because the total number of order parameters that are determined is larger than that directly calculable from the individual probe data sets. In addition, because the relationships between the fluorescent and spin probes are known (i.e., the Euler angles relating the probe fixed reference frames are known), the fluorescent probe order parameters of rank $j > 4$ (that cannot be directly detected by fluorescence intensities) can be calculated by rotating the appropriate spin probe order parameters. We use our ability to do this in the accompanying paper where fluorescent probe angular distributions are shown that include contributions from rank $j = 6$ order parameters.

We demonstrate advantage (iii) again in the accompanying paper where the Euler angles relating the probe-fixed reference frames are used to plot the angular trajectory of the absorption and emission dipoles of 15IA as a function of excitation wavelength. The ability to experimentally rotate these dipoles using wavelength variation (either excitation or emission) is critical to the demonstration that rigor cross-bridges rotate upon binding MgADP (Ajtai & Burghardt, 1987). Visualizing the orientation of the dipoles in space aids us in suggesting models for muscle contraction.

Work in progress uses this global approach for mapping probe movements to (i) extend resolution of the probe angular distribution to the order parameters $j = 1$ and 3 and (ii) investigate the internal flexibility of the myosin cross-bridge. Extending the method to estimate the $j = 1$ and 3 probe order parameters is a matter of measuring the fluorescence polarization intensities for a larger set of excitation and emission polarizer orientations. These odd rank order parameters could be important in muscle contraction since they break the symmetry in which probe distributions are unaltered by the coordinate transformation $(\beta,\gamma) \rightarrow (\pi-\beta,\pi+\gamma)$.

One approach for investigating the internal flexibility of myosin would be to use data from EPR and fluorescent probes on spatially separated sites on the myosin cross-bridge. Our analysis of multiple probes presumes that the cross-bridge rotates as a rigid body. The correctness of this assumption is tested by whether or not data from spatially separated probes are consistent with the rigid body rotation of the probe host. We have methods for placing probes on myosin SH1 and SH2. SH1 and SH2 will serve as the spatially separated probe sites on which to base this analysis.

Appendix

The fluorescence intensities are identified by wavelength (both excitation, λ_{ex} and emission, λ_{em}) and by the polarization of the electric fields of the exciting and emitted light. Figure 3 shows the lab frame with exciting light of wavelength λ_{ex} propagating along the y-axis with the linearly polarized electric field orientation given by $\vec{E}_{ex}$, such that

$$\vec{E}_{ex} = E_0(-\sin\psi, 0, \cos\psi) \quad \text{(A1)}$$

where E_0 is a scalar independent of polarization. Emitted light, propagating along the x-axis, is linearly polarized along $\vec{n}$ by the emission polarizer and passes through a filter or monochromator to select the emission wavelength, λ_{em}. The orientation of the emitted light polarization, $\vec{n}$, is given by

$$\vec{n} = (0, \sin\chi, \cos\chi) \quad \text{(A2)}$$

The relationship between the fluorescence intensity $F(\psi,\chi,\lambda_{ex},\lambda_{em})$ and the probe order parameters is given by

formulae derived previously in a more general form (Burghardt, 1984). It can be shown that if the probe transition dipoles in the probe fixed frame are assumed to be of the form

$$\vec{\mu}_a = (0, 0, 1) \quad \text{(A3)}$$

$$\vec{\mu}_e = (\sin\theta, 0, \cos\theta) \quad \text{(A4)}$$

and if $\mathbf{v}$ is a 25×1 array made from the fluorescent probe order parameters such that

$$\mathbf{v} = \{a^0_{0,0}, a^1_{0,0}, (a^1_{0,1} + a^1_{0,-1})/(2i), (a^1_{0,1} - a^1_{0,-1})/2, a^2_{0,0}, (a^2_{0,1} + a^2_{0,-1})/(2i), (a^2_{0,1} - a^2_{0,-1})/2, (a^2_{0,2} + a^2_{0,-2})/2, (a^2_{0,2} - a^2_{0,-2})/(2i), a^3_{0,0}, (a^3_{0,1} + a^3_{0,-1})/(2i), (a^3_{0,1} - a^3_{0,-1})/2, (a^3_{0,2} + a^3_{0,-2})/2, (a^3_{0,2} - a^3_{0,-2})/(2i), (a^3_{0,3} + a^3_{0,-3})/(2i), (a^3_{0,3} - a^3_{0,-3})/2, a^4_{0,0}, (a^4_{0,1} + a^4_{0,-1})/(2i), (a^4_{0,1} - a^4_{0,-1})/2, (a^4_{0,2} + a^4_{0,-2})/2, (a^4_{0,2} - a^4_{0,-2})/(2i), (a^4_{0,3} + a^4_{0,-3})/(2i), (a^4_{0,3} - a^4_{0,-3})/2, (a^4_{0,4} + a^4_{0,-4})/2, (a^4_{0,4} - a^4_{0,-4})/(2i)\} \quad \text{(A5)}$$

then

$$F(\psi,\chi,\lambda_{ex},\lambda_{em}) = \mathbf{B}\mathbf{v} \quad \text{(A6)}$$

$$\mathbf{B} = (8\pi^2)^{1/2}\{1/9, 0, -i/(2/5)b(1)\sin\theta\cos\theta, 0, (1/5)^{1/2}[(2/9)(\cos^2\psi - 0.5\sin^2\psi)(\cos^2\chi - \sin^2\chi) + (2/3)^{1/2}[f - /(2/7)b(2)](\cos^2\theta - 0.25\sin^2\theta)], 0, (1/5)^{1/2}\sin\theta\cos\theta[(2/7)^{1/2}b(2) - 2f], (1/5)^{1/2}\sin^2\theta[f + (2/7)^{1/2}b(2)], 0, 0, (4/35)^{1/2}ib(3)\sin\theta\cos\theta, 0, 0, -(1/14)^{1/2}ib(3)\sin^2\theta, 0, 0, (4/105)^{1/2}b(4)(\cos^2\theta - 0.25\sin^2\theta), 0, -(4/21)^{1/2}b(4)\sin\theta\cos\theta, (1/42)^{1/2}b(4)\sin\theta, 0, 0, 0, 0, 0\} \quad \text{(A7)}$$

$$f = (1/3)(1/6)^{1/2}(2 - 3\sin^2\chi) \quad \text{(A8)}$$

$$b(j) = \langle 2,2,0,0|j,0\rangle(2/27)^{1/2}(\cos^2\psi - 0.5\sin^2\psi) \times (2 - 3\sin^2\chi) + 0.25(2/3)^{1/2}\sin^2\psi\sin^2\chi(\langle 2,2,-2,2|j,0\rangle - \langle 2,2,2,-2|j,0\rangle) + i(2/3)^{1/2}\sin\psi\cos\psi\sin\chi\cos\chi \times (\langle 2,2,-1,1|j,0\rangle - \langle 2,2,1,-1|j,0\rangle) \quad \text{(A9)}$$

$i = \sqrt{-1}$, and $\langle j_1,j_2,m_1,m_2|j,m\rangle$ is the Clebsch–Gordon coefficient (Davydov, 1963). Inspection of eq A9 shows that if ψ or χ equals 0° or 90° then $b(j = 1) = b(j = 3) = 0$, implying that the $j = 1$ and 3 order parameters do not contribute to the fluorescent intensity. As mentioned in the text, one must select values for ψ and χ different from 0° and 90° to be able to use the fluorescence polarization data to solve for the $j = 1$ and 3 order parameters.

The expression for F in equs A5–A9 is substituted into eqs 9, 10, and 11 to form equations relating fluorescent probe order parameters to the observable polarization ratios. Order parameters $\mathbf{v}$ are related to the spin probe order parameters $\mathbf{u}$ by an appropriate rotation of the form of eq 3. The combination of these relationships leads to eq 13 and the explicit expression for the elements of matricies $\mathbf{G}$ and $\mathbf{k}_f$.

Registry No. MgADP, 7384-99-8.

References

Ajtai, K., & Burghardt, T. P. (1987) *Biochemistry 26*, 4517–4523.

Ajtai, K., Ringler, A., & Burghardt, T. P. (1992) *Biochemistry* (following paper in this issue).

Borejdo, J., Assulin, O., Ando, T., & Putnam, S. (1982) *J. Mol. Biol. 158*, 391–414.

Burghardt, T. P. (1984) *Biopolymers 23*, 2383–2406.

Burghardt, T. P. (1989) *Chem. Phys. Lipids 50*, 271–287.

Burghardt, T. P., & Thompson, N. L. (1985) *Biophys. J. 48*, 401–409.

Burghardt, T. P., & French, A. R. (1989) *Biophys. J. 56*, 525–534.

Burghardt, T. P., & Ajtai, K. (1990) in *Molecular Mechanisms in Muscular Contraction* (Squire, J., Ed.) pp 211–239, MacMillan, London.

Burghardt, T. P., Ando, T., & Borejdo, J. (1983) *Proc. Natl. Acad. Sci. U.S.A. 80*, 7515–7519.

Cooke, R., Crowder, M. S., & Thomas, D. D. (1982) *Nature (London) 300*, 776–778.

Davydov, A. S. (1963) *Quantum Mechanics*, p 145, NEO Press, Ann Arbor, MI.

Fajer, P. G., Fajer, E. A., Matta, J. J., & Thomas, D. D. (1990) *Biochemistry 29*, 5865–5871.

Haskell, H. H., & Hanson, R. J. (1979) Report SAND 78-1290, Sandia Laboratories, Albuquerque, NM.

Huxley, A. F. & Simmons, R. M. (1971) *Nature (London) 233*, 533–538.

Huxley, H. E. (1969) *Science 164*, 1356–1366.

Robinson, B. H., Thomann, H., Beth, A. H., Fajer, P., & Dalton, L. R. (1985) in *EPR and Advanced EPR Studies of Biological Systems* (Dalton, L. R., Ed.) pp 111–182, CRC Press, Boca Raton, FL.

Strang, G. (1986) *Introduction to Applied Mathemetics*, pp 87–137, Wellesley-Cambridge Press, Wellesley MA.